TÜBİTAK

Research Article

Turk J Agric For
36 (2012) 510-517
© TÜBİTAK
doi:10.3906/tar-1105-4

Effects of compatibilizer and nanolayered silicate on physical and mechanical properties of PP/bagasse composites

Behzad KORD*

Department of Wood Science and Paper Technology, Islamic Azad University, Chalous Branch, PO Box 46615/397, Mazandaran - IRAN

Received: 03.05.2011 ● Accepted: 15.01.2012

Abstract: Bagasse, an agricultural waste, was investigated for wood plastic nanocomposite production. The incorporation of nanolayered silicate has been considered in recent years for improving the properties of thermoplastic composite. In this study a composite of polypropylene (PP) and bagasse fiber (BF), with different concentrations of nanoclay and maleic anhydride (MA) as compatibilizer, were fabricated by injection molding. Then physical and mechanical properties of the composites were tested according to ASTM standards. The results indicated that tensile modulus and flexural strength increased with an increase in clay loading; however, impact strength and water absorption decreased with an increase in nanolayered silicates. The degree of nanoclay dispersion in PP/BF composite was characterized by X-ray diffraction (XRD) method. The morphological study showed that the intercalation morphology in nanocomposite samples and d-spacing of layers increased with an increase in clay content. The effect of compatibilizer was positive in terms of enhancing the properties of composites. The maximum physical and mechanical properties of samples were achieved with 3% nanolayered silicates and 2% coupling agent.

Key words: Bagasse, compatibilizer, injection molding, nanolayered silicates, polypropylene

Introduction

The global wood plastic composites (WPC) market has been experiencing double digit growth since 2003, with a similar trends projected up to 2010. Current product lines include lumber, decking and railing, window profiles, wall studs, door frames, furniture, pallets, fencing, docks, siding, architectural profiles, and automotive components (Kiguchi 2007).

With increasing wood costs and competition for wood resources among traditional wood sectors, developing alternative, environmentally friendly fiber sources for plastic composites is crucial (Han et al. 2008). Moreover, enforcement of new and stricter environmental policies has forced industries to search for new materials to replace the traditional composite materials, which use a plastic matrix and inorganic fillers as reinforcement. Compared to traditional synthetic fillers, natural filler/fibers (e.g., kenaf fiber, wood flour, hemp, sisal) present lower density, less abrasiveness, and lower cost; they are also renewable and biodegradable (Rowel et al. 1997).

Sugarcane bagasse is abundantly available in many countries. In 2009, 817 million tons of bagasse was produced worldwide. It is a by-product of many agricultural activities, and it is suitable for the production of energy, ethanol, animal feeds, paper products, composite board, and building materials. It is also used as a feedstock for the fluidized bed

* E-mail: behzad_k8498@yahoo.com

production of a range of chemicals (Nourbakhsh and Kouhpayehzadeh 2009). Bagasse is one of the most important lignocellulosic raw materials in Iran. It is estimated that about 1.2 million tons of bagasse is produced in Iran annually. During the last few decades, much effort has been devoted to increasing the utilization of bagasse; however, large quantities of this raw material are still left unused or burnt (Zabihzadeh 2010).

A relatively simple possibility is to use bagasse as reinforcing filler for thermoplastic composites. Bagasse-based thermoplastic composites can replace wood in applications such as furniture and interior panels. The potential utilization of this material for traditional composite panel manufacture has been explored (Nourbakhsh and Kouhpayehzadeh 2009).

The enhancement of material properties achieved by including submicron-sized fillers [e.g., montmorillonite (MMT) clay, which consists of silicate layers] in plastics and elastomers has stimulated research in polymer composites. Different polymer/clay nanocomposites have been successfully prepared by incorporating clay in polymer matrixes such as polyimide, PP, epoxy, and polystyrene (Tjong 2006; Viswanathan et al. 2006; Utracki et al. 2007). Clay nanocomposites, especially nanoclay/polymer composites, exhibit dramatic increases in modulus, strength, barrier properties, flammability resistance, and heat resistance compared with conventional or microcomposites (Wang et al. 2001; Boukerrou et al. 2007; Chen et al. 2007; Lei et al. 2007; Wu et al. 2007; Hetzer and Kee 2008).

This study has 2 purposes: (1) to investigate the feasibility of using bagasse as a reinforcement material for polypropylene (PP) composites and (2) to determine the effect of a coupling agent on clay dispersion and mechanical properties of the composites.

Materials and methods

Materials

Bagasse was collected from sugarcane fields in the south of Iran (Ahvaz, Khuzestan). Polypropylene homopolymer, which has a melt flow index of 4 g/10 min and a density of 0.9 g/cm^3, was supplied by Arak Petrochemical Industries, Iran; it was used in this work as the polymer matrix. Maleic anhydride (MA) (Merck, Frankfurt, Darmstadt, Germany) was used as coupling agent and dicumyl peroxide (DCP) (the initiator) was supplied by Hercules (Wilmington, DE, USA). Irganox 1010, supplied by Ciba, was also added to the composite as a heat stabilizer. Cloisite 30B, a natural montmorillonite modified with a methyl, tallow, bis-2-hydroxyethyi, quaternary ammonium [cationic exchange capacity (CEC) = 90 meq/100 g clay, d-spacing (d_{001}) = 18.5 Å] was obtained from Southern Clay Products. It is supplied in a particulate form with sizes in the micro scale range (10% less than 2 μm, 50% less than 6 μm, and 90% less than 13 μm).

Methods

Composite manufacturing

Before sample preparation the bagasse was chopped by laboratory chopper and soaked in tap water for 1 h. Then the soaked bagasse was steamed under 8 bar pressure at 170 °C. The steamed bagasse was then pulped by a laboratory atmospheric refiner. The pulp was gradually collected and predried. The drying process was completed in a convective oven at 100 °C. After drying, the dry-basis moisture content of fiber ranged from 2% to 3%. Then the PP, bagasse fiber (BF), nanoclay, and coupling agent (MA) were weighed and bagged according to the formulations given in Table 1. The mixing was by Hake internal mixer (Model HBI System 90, USA) at 180 °C and 60 rpm. First, the PP was fed into the mixing chamber, and after melting the PP and coupling agent, DCP and nanoclay were added. At 5 min the BF was fed; total mixing time was 13 min. The compounded materials were then ground using a pilot scale grinder (Wieser, WGLS 200/200 model). The resulting granules were dried at 105 °C for 4 h. Test specimens were prepared by injection molding (Eman Machine, Iran). Prior to testing, specimens were conditioned at 23 °C and a relative humidity of 50% for at least 40 h, according to ASTM D618-99.

Testing procedure

The degree of nanoclay intercalation in composites was characterized by X-ray diffraction (XRD). XRD measurements taken on powdered nanoclay and nanocomposites were carried out with a Seifert 3003 PTS (Germany) using CuKα radiation (λ = 1.54 nm);

Table 1. Composition of the studied formulations.

Samples	Polypropylene content (Wt. %)	Bagasse fiber content (Wt. %)	Nanolayered silicate content (Wt. %)	Compatibilizer content (Wt. %)
1	40	60	0	0
2	38	60	0	2
3	40	59	1	0
4	38	59	1	2
5	40	58	2	0
6	38	58	2	2
7	40	57	3	0
8	38	57	3	2

the generator power was 50 kV and 50 mA. The scan mode was continuous, with a scan rate of 1°/min in scan range from 0° to 12°.

The tensile and flexural tests were carried out using an Instron machine (model 1186, England) at test speed of 2 mm/min to ASTM standards D638 and D790, respectively. A Zwick impact tester (model 5102, Germany) was used for the Izod impact test. All the samples were notched on the center of 1 longitudinal side, according to ASTM D256. Water absorption tests were carried out according to ASTM D 7031 specifications. From each formulation, 5 specimens were selected and dried in an oven for 24 h at 102 °C ± 3 °C. The weight and thickness of dried specimens were measured to a precision of 0.001 g and 0.001 mm, respectively. The specimens were then placed in distilled water and kept at room temperature. For each measurement, specimens were removed from the water and surface water was wiped off using blotting paper. The weight of the specimens was measured after 24 h. The water absorption values, as percentages, were calculated using the following equation:

$$WA_{(t)} = \frac{W_{(t)} - W_0}{W_0} \times 100 \quad (1)$$

where WA (t) is the water absorption at time, t; W_0 is the oven dried weight; and W (t) is the weight of specimen at a given immersion time, t.

This research was carried out in a completely randomized design, and 5 replications for all tests were considered. To analyze the data, 1-way analysis of variance (ANOVA) was employed, and Duncan's multiple range test (DMRT) was used to group the means. All comparisons were performed at a 95% confidence level.

Results

Statistical analysis indicated that the nanolayered silicate and coupling agent content had significant effects ($P < 0.05$) on the physical and mechanical properties of PP/BF composites (Tables 2 and 3).

Figure 1 shows the variation of the tensile modulus versus nanolayered silicate loading at different levels of coupling agent in PP/BF composites. The addition of nanolayered silicate increased the tensile modulus of PP/BF composites. Figure 1 also shows that the tensile modulus of composites increases with an increase in MA at different levels of nanolayered silicate.

Figure 2 illustrates the flexural strengths of samples versus nanolayered silicate loading at different levels of coupling agent in PP/BF composites. The variation in flexural strength of PP/BF composites was similar to tensile modulus; a maximum flexural strength was observed at 3% nanolayered silicate and 2% MA.

Figure 3 shows variation in impact strength versus nanolayered silicate loading at different levels of

Table 2. Statistical analysis of variance (ANOVA) for effect of nanolayered silicate on the physical and mechanical properties of PP/BF composites.

Property		Sum of squares	df	Mean square	F	Sig.
Tensile modulus	between groups	4377186.333	3	1459062.111	12.201	0.000*
	within groups	2391681.000	20	119584.050		
	total	6768867.333	23			
Flexural strength	between groups	68.997	3	22.999	0.838	0.039*
	within groups	548.580	20	27.429		
	total	617.577	23			
Impact strength	between groups	74.967	3	24.989	4.655	0.013*
	within groups	107.363	20	5.368		
	total	182.330	23			
Water absorption	between groups	2.054	3	0.685	1.555	0.002*
	within groups	8.808	20	0.440		
	total	10.862	23			

*: significant difference between samples ($P < 0.05$).

Table 3. Statistical analysis of variance (ANOVA) for effect of coupling agent on the physical and mechanical properties of PP/BF composites.

Property		Sum of squares	df	Mean square	F	Sig.
Tensile modulus	between groups	394753.500	1	394753.500	1.362	0.006*
	within groups	6374113.833	22	289732.447		
	total	6768867.333	23			
Flexural strength	between groups	130.807	1	130.807	5.912	0.024*
	within groups	486.770	22	22.126		
	total	617.577	23			
Impact strength	between groups	30.398	1	30.398	4.402	0.038*
	within groups	151.933	22	6.906		
	total	182.330	23			
Water absorption	between groups	1.362	1	1.362	3.155	0.019*
	within groups	9.499	22	0.432		
	total	10.862	23			

*: significant difference between samples ($P < 0.05$).

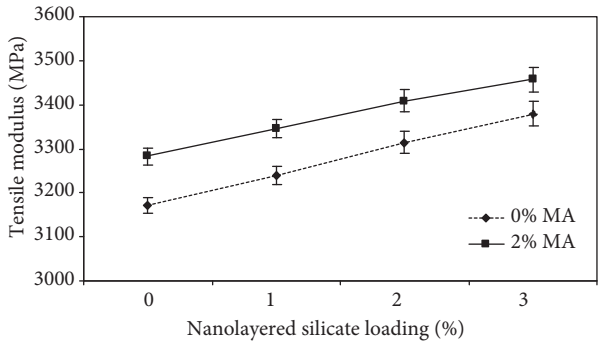

Figure 1. Effect of nanolayered silicate and coupling agent on tensile modulus of PP/BF composites.

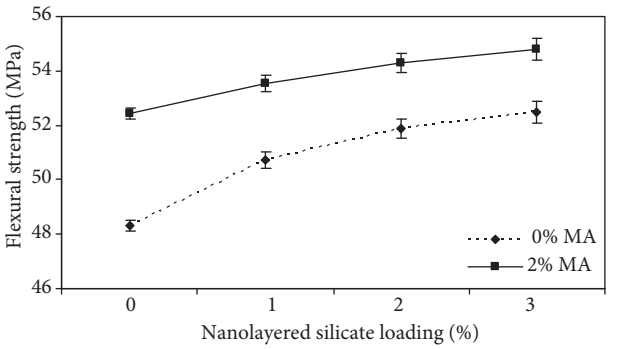

Figure 2. Effect of nanolayered silicate and coupling agent on flexural strength of PP/BF composites.

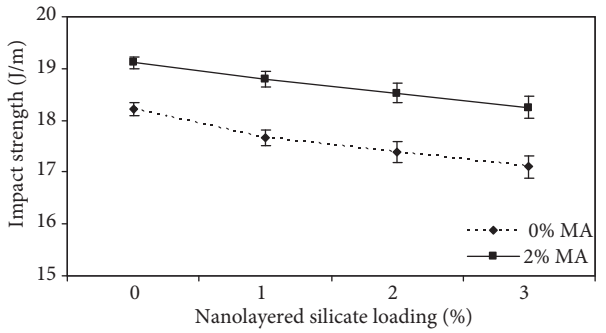

Figure 3. Effect of nanolayered silicate and coupling agent on impact strength of PP/BF composites.

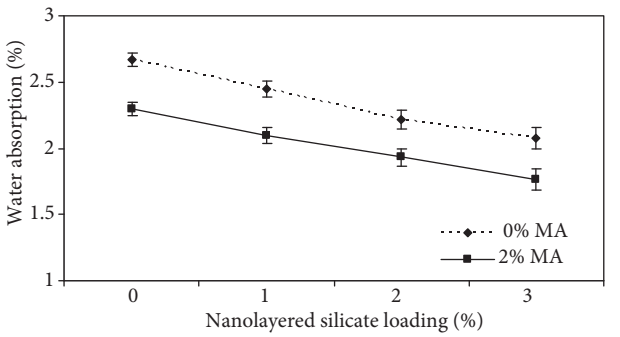

Figure 4. Effect of nanolayered silicate and coupling agent on water absorption of PP/BF composites.

coupling agent in PP/BF composites. The addition of nanolayered silicate decreased impact strength of PP/BF composites. Figure 3 also shows that the impact strength increased with increase in MA at different levels of nanolayered silicate.

Figure 4 shows the variation in water absorption versus nanolayered silicate loading at different levels of coupling agent in PP/BF composites. The water absorption of PP/BF composites decreased with an increase in nanolayered silicate loading. Figure 4 also shows that water absorption decreases by adding MAPP.

Characterization of the morphological state of the composites was accomplished using XRD. To verify a homogeneous dispersion of nanoclay (so-called intercalation and exfoliation) in a polymer matrix the interlayer spacing in nanolayered silicates (Bragg's law) and the relative intercalation (RI) of the polymer in nanoclay were quantified using the following equations:

$$n\,\lambda = 2d \sin\theta \tag{2}$$

$$RI = [(d - d_o) \div d_o] \times 100, \tag{3}$$

where n is the integer number of wavelength (n = 1), λ is the wavelength of the X-rays, d is the interlayer or d-spacing of the clay in the nanocomposite, θ is half of the angle of diffraction, and d_o is the spacing of the clay layers in the pristine clay.

The d-spacing and relative intercalation of the clay in the nanocomposites calculated from equations 1 and 2 are listed in Table 4. The peaks appearing at 4.77° correspond to powdered nanoclay with d_{001} = 18.5 nm. In the sample with the addition of 1% nanoclay, the peak was shifted to a lower angle (2θ = 3.96°, d_{001} = 22.3 nm), which implies formation of the intercalation morphology. This means that the interlayer distance and relative intercalation of clay increased. Moreover, significant reduction in the

Table 4. Interlayer spacing and relative intercalation in PP/BF nanocomposites.

Samples	2θ (°)	d-spacing (nm)	Relative intercalation (%)
Pristine nanolayered silicate	4.77	18.5	-
C + 1% NC	3.96	22.3	20.54
C + 1% NC + 2% MA	3.43	25.7	38.92
C + 2% NC	3.58	24.6	32.97
C + 2% NC + 2% MA	3.14	28.1	51.89
C + 3% NC	3.46	25.5	37.84
C + 3% NC + MA 2% MA	3.02	29.2	57.84

*C: composite, NC: nanoclay without coupling agent, NC + MA: nanoclay with coupling agent.

diffraction peak intensity was observed by increasing the nanolayered silicate loading. However, the clay was not exfoliated since the peak clearly still existed. These data show that the order of intercalation was higher for 3% of nanoclay (2θ = 3.46°, d_{001} = 25.5 nm). In other words, formation of the intercalation morphology and better dispersion was shown at 3% nanoparticles, because the peak of sample with 3% of nanoclay was shifted to a lower angle. As shown in Table 2, with the addition of MA in the composite the d-spacing and relative intercalation of the nanolayered silicate increased.

Discussion

It is well known that nanoclay particles with a very high aspect ratio can improve the modulus of the PP (Boukerrou et al. 2007; Chen et al. 2007; Han et al. 2008). The increase in properties may also be attributed to the intercalated and exfoliated nanocomposite structures formed at these loadings of clay (Wang et al. 2001; Lei et al. 2007; Wu et al. 2007; Han et al. 2008). It is well established that coupling agents enhance the interface adhesion between wood flour and PP matrix, which results in better encapsulation of wood particles by the plastic, creating a higher tensile modulus (Raj et al. 1989; Kokta et al. 1990; Guduri et al. 2007). In addition, the coupling agent improves adhesion within the interphase between polymer matrix and nanoclay-layered silicate.

The decrease in impact strength at higher nanoclay content levels is probably due to the formation of clay agglomeration and the presence of unexfoliated aggregates and voids (Yuan and Misra 2006; Zhao et al. 2006). The enhancement of impact strength with increasing MA could be attributed to the more homogeneous dispersion of the fiber, which is the result of increasing fiber wettability as concentration of the coupling agent increases; this leads to more uniform distribution of the applied stress. As a result, more energy is required for fiber debonding and subsequent fiber pull-out, the causes of composite impact failure.

It seems that the barrier properties of nanoclay fillers inhibited water permeation in the polymer matrix, and 2 mechanisms have been reported for this phenomenon. The first is based on the hydrophilic nature of the clay surface, which tends to immobilize some of the moisture (Rana et al. 2005). The second mechanism is based on surfactant-covered clay platelets forming a tortuous path for water transport (Alexandre et al. 2006). This barrier property hinders water from entering the inner part of the nanocomposite. Another reason for lower moisture content could be the change in crystallinity of the composite when nanoclay functions as a nucleating agent (Bharadwaj et al. 2002). The nucleation efficiency and the crystallinity of the hybrid composite can be improved by the presence of nanofiller as a nucleating agent. As the crystalline regions are impermeable, water

absorption is lower in the composites. Generally, it is necessary to use compatibilizers or coupling agents in order to improve the polymer/fiber bonding and enhance water resistance. The MA chemically bonds with the OH groups in the lignocellulosic filler and limits the water absorption and thickness swelling of composites. As a result, it is important to use coupling agents to improve the quality of adhesion between plastics and fibers, reduce gaps in interfacial region, and block the hydrophilic groups.

The increase in interlayer distance and relative intercalation might result from the stronger shear that emerged during processing when BF was introduced. Coupling agent (MA) molecules could enter and penetrate the gallery between clay layers when the clay was mixed with MA. The driving force responsible for penetration originated in the strong hydrogen bonding between the maleic anhydride group (or COOH group, generated from the hydrolysis of the maleic anhydride group) and the oxygen groups of the silicates (Zhao et al. 2006; Han et al. 2008). The addition of a coupling agent caused interlayer spacing of the clay to increase, and therefore the interaction of the layers should be weakened. In other words, by improving the compatibility between polymer matrix and clay (using MA), the polymer chains can be well diffused into the clay layers, and the basal spacing of clay layers may increase (Kord et al. 2011). In the case of polymers containing polar functional groups, alkyl ammonium surfactant-modified nanolayered silicate is adequate to promote nanocomposite formation. Kord et al. (2011) found that by increasing nanoclay to 6 phc, the size of dispersed nanoclay became larger or even aggregated in part, and the presence of coupling agent improved the dispersion of nanoclay as the clay aggregates were broken down into smaller stacks.

Conclusions

The following conclusions were obtained from this research:

1. The tensile modulus and flexural strength increased with an increase in nanolayered silicate loading. However, the impact strength and water absorption decreased with an increase in nanolayered silicates.
2. The degree of nanoclay dispersion in the BF-filled PP composites was characterized by XRD method. The morphological study showed that the intercalation morphology in nanocomposite samples, as well as the d-spacing and relative intercalation of layers, increased with increasing clay content.
3. Physical and mechanical properties of the composites were improved by compatibilizer loading.
4. With the addition of MA to the composite, the d-spacing and relative intercalation of the nanolayered silicate increased.
5. The maximum physical and mechanical properties of samples were achieved with 3% nanolayered silicates and 2% coupling agent.

References

Alexandre B, Marais S, Langevin S, Médéric P, Aubry T (2006) Nanocomposite-based polyamide 12/montmorillonite: relationships between structures and transport properties. Desalini J 99: 164-166.

Bharadwaj RK, Mehrabi AR, Hamilton C, Trujillo C, Murga M, Fan R, Chavira A, Thompson AK (2002) Structural property relationship crosslinked polyester clay nanocomposites. Polym J 43: 3699-3705.

Boukerrou A, Duchet J, Fellahi S, Kaci M, Sautereau H (2007) Morphology and mechanical and viscoelastic properties of rubbery epoxy/organoclay montmorillonite nanocomposites. J Appl Polym Sci 103: 3547-3552.

Chen H, Wang M, Lin Y, Chan CM, Wu J (2007) Morphological and mechanical property of binary polypropylene nanocomposites with nanoclay particles. J Appl Polym Sci 103: 4451-4458.

Guduri BR, Luyt AS (2007) Comparison of the influence of different compatibilizers on the structures and properties of ethylene vinyl acetate copolymer/modified clay nanocomposites. J Appl Polym Sci 103: 1268-1274.

Han G, Lei Y, Wu Q, Kojima Y, Suzuki S (2008) Bamboo-fiber filled high density polyethylene composites: effect of coupling treatment and nanoclay. J Polym Environm 21: 1567-1582.

Hetzer M, Kee D (2008) Wood/polymer/nanoclay composites, environmentally friendly sustainable technology: a review. J Chem Eng 16: 1016-1027.

Kiguchi M (2007) Latest markets of wood and wood plastic composites in North America and Europe. In: Second Wood and Wood Plastic Composites Seminar in the 23rd Wood Composite Symposium. Kyoto, Japan: pp. 61-73.

Kokta BV, Beland P, Maldas D (1990) Improving adhesion of wood fiber with polystyrene by chemical treatment of fiber with coupling agent and influence on mechanical properties. J Compos 3: 529-539.

Kord B, Hemmasi A, Ghasemi I (2011) Properties of PP/wood flour/organomodified montmorillonite nanocomposite. Wood Sci Technol 45: 111-119.

Lei Y, Wu Q, Clemons CM, Yao F, Xu Y (2007) Influence of nanoclay on properties of HDPE/wood composites. J Appl Polym Sci 18: 1425-1433.

Nourbakhsh A, Kouhpayehzadeh M (2009) Mechanical properties and water absorption of fiber-reinforced polypropylene composites prepared by bagasse and beech fiber. J Appl Polym Sci 114: 653-657.

Raj RG, Kokta BV (1989) Effect of chemical treatment of fiber composites. J Adhes Sci Technol 3: 55-64.

Rana HT, Gupta RK, Ganga Rao HVS, Sridhar LN (2005) Measurement of moisture diffusivity through layered-silicate nanocomposites. AIChE J 51: 3249-3256.

Rowell RM, Sandi AR, Gatenholm DF, Jacobson RE (1997) Utilization of natural fibers in plastic composites: problems and opportunities in lignocellulosic composites. J Compos 18: 23-51.

Tjong SC (2006) Structural and mechanical properties of polymer nanocomposites: a review. J Mater Sci Eng 53: 73-197.

Utracki LA, Sepehr M, Boccaleri E (2007) Synthetic layered nanoparticles for polymeric nanocomposites (PNCs): a review. J Polym Adv Technol 18: 1-37.

Viswanathan V, Laha T, Balani K, Agarwal A, Seal S (2006) Challenges and advances in nanocomposite processing techniques: a review. J Mater Sci Eng 54: 121-285.

Wang KH, Choi MH, Koo CM, Choi YS, Chung IJ (2001) Synthesis and characterization of maleated polyethylene/clay nanocomposites. J Polym 42: 9819-9826.

Wu Q, Lei Y, Clemons CM, Yao F, Xu Y, Lian K (2007) Properties of HDPE/clay/wood nanocomposites. J Plast Technol 27: 108-115.

Yuan Q, Misra RDK (2006) Impact fracture behavior of clay-reinforced polypropylene nanocomposites. J Appl Polym Sci 47: 4421-4433.

Zabihzadeh SM (2010) Flexural properties and orthotropic swelling behavior of bagasse/thermoplastic composites. BioResou 5: 650-660.

Zhao Y, Wang K, Zhu F, Xue P, Jia M (2006) Properties of poly(vinyl chloride)/wood flour/montmorillonite composites: effects of coupling agents and layered silicate. Polym Degrad Stabil 91: 2874-2883.